

A Rapid Fluorescence Assay for FtsZ Assembly Indicates Cooperative Assembly with a Dimer Nucleus

Yaodong Chen,* Keith Bjornson,[†] Samba D. Redick,* and Harold P. Erickson*

*Departments of Cell Biology and [†]Biochemistry, Duke University Medical Center, Durham, North Carolina

ABSTRACT FtsZ is the major cytoskeletal protein operating in bacterial cell division. FtsZ assembles into protofilaments *in vitro*, and there has been some controversy over whether the assembly is isodesmic or cooperative. Assembly has been assayed previously by sedimentation and light scattering. However, these techniques will under-report small polymers. We have now produced a mutant of *Escherichia coli* FtsZ, L68W, which gives a 250% increase in tryptophan fluorescence upon polymerization. This provides a real-time assay of polymer that is directly proportional to the concentration of subunit interfaces. FtsZ-L68W is functional for cell division, and should therefore be a valid model for studying the thermodynamics and kinetics of FtsZ assembly. We assayed assembly at pH 7.7 and pH 6.5, in 2.5 mM EDTA. EDTA blocks GTP hydrolysis and should give an assembly reaction that is not complicated by the irreversible hydrolysis step. Assembly kinetics was determined with a stopped-flow device for a range of FtsZ concentrations. When assembly was initiated by adding 0.2 mM GTP, fluorescence increase showed a lag, followed by nucleation, elongation, and a plateau. The assembly curves were fit to a cooperative mechanism that included a monomer activation step, a weak dimer nucleus, and elongation. Fragmentation was absent in the model, another characteristic of cooperative assembly. We are left with an enigma: how can the FtsZ protofilament, which appears to be one-subunit thick, assemble with apparent cooperativity?

INTRODUCTION

FtsZ provides the framework for the cytokinetic ring that powers bacterial cell division. The Z ring has been visualized at the light microscope level using immunofluorescence and green fluorescent protein tagged FtsZ (Levin and Losick, 1996; Ma et al., 1996; Sun and Margolin, 1998; Stricker and Erickson, 2003; Anderson et al., 2004), but its substructure has not been resolved by electron microscopy (EM) of bacteria. *In vitro* *Escherichia coli* FtsZ assembles into thin protofilaments that can exist either as single protofilaments or as small sheets or bundles (Erickson et al., 1996; Mukherjee and Lutkenhaus, 1999; Romberg et al., 2001). It is thought that these protofilaments are the building block for the Z ring *in vivo*.

Assembly of FtsZ *in vitro* has been studied by EM, centrifugation, light scattering, and isothermal titration calorimetry (Erickson et al., 1996; Mukherjee and Lutkenhaus, 1999; Caplan and Erickson, 2003; Gonzalez et al., 2003; Oliva et al., 2003). Each of these techniques presents problems for quantitative analysis. EM is not quantitative, and sedimentation will not capture small polymers. Sedimentation and calorimetry are slow techniques and cannot be used for kinetics. Light scattering has the advantage of providing a real-time measure of assembly, but it cannot be used as a quantitative measure of total polymer because

small polymers are under-reported, and association of protofilaments into bundles would cause a large increase in light scattering for the same polymer mass.

Trusca and Bramhill (2002) recently described a fluorescence assay for FtsZ assembly suitable for rapid throughput screening using a 96-well format. This assay used DEAE dextran to stabilize polymers, which were then collected by filtration through a nylon membrane. We have found that several mutants of FtsZ that are blocked for assembly are nevertheless precipitated by adding DEAE dextran. This assay might therefore fail to report some conditions or reagents that block FtsZ assembly but permit aggregation in the presence of DEAE dextran.

The study of actin polymerization was enormously advanced by the discovery that pyrene-labeled actin gave a substantial increase in fluorescence upon assembly (Kouyama and Mihashi, 1981; Cooper et al., 1983b). Careful studies showed that the fluorescence increase was directly proportional to the amount of pyrene actin in polymer. The pyrene fluorescence thus gave a real-time readout of the actin in polymer. This assay has been used in numerous studies to determine the kinetics of actin polymerization, and the kinetics were fit to mechanisms with a dimer and/or trimer nucleus (Cooper et al., 1983a; Frieden, 1983; Frieden and Goddette, 1983; Tobacman and Korn, 1983; Buzan and Frieden, 1996).

We now report the discovery of a mutant of *E. coli* FtsZ, L68W, which produces a 250% increase in tryptophan fluorescence upon assembly. The L68W mutant, which is located on the upper protofilament interface near the GTP, was originally designed to be a steric block of protofilament

Submitted April 8, 2004, and accepted for publication October 4, 2004.

Address reprint requests to Harold P. Erickson, Tel.: 919-684-6385; E-mail: h.erickson@cellbio.duke.edu.

Keith Bjornson's present address is CEPTYR Inc., 3830 Monte Villa Parkway, Bothell, WA 98021.

Samba Redick's present address is Program in Molecular Medicine, University of Massachusetts Medical School, Worcester, MA.

© 2005 by the Biophysical Society

0006-3495/05/01/505/10 \$2.00

doi: 10.1529/biophysj.104.044149

assembly. However, we found that it was functional for cell division, and assembled normally in vitro (S. D. Redick, J. Stricker, G. Briscoe and H. P. Erickson, unpublished). We then investigated its fluorescence and discovered that it was an excellent reporter of assembly. We have used it in the present study to determine the thermodynamics and kinetics of FtsZ assembly in vitro.

MATERIALS AND METHODS

FtsZ-L68W purification

The mutant L68W of *E. coli* FtsZ was overexpressed from a pET11b vector (Novagen, Madison, WI). The protein L68W was purified using the protocol of Romberg et al. (2001), with some modification. After the 20% ammonium sulfate cut and 30% precipitation, the protein was chromatographed on a Resource Q 10/10 column (Amersham Biosciences, Piscataway, NJ) with a linear gradient of 100 mM to 500 mM KCl in 50 mM Tris, pH 7.9, 1 mM EDTA, 10% glycerol. The protein was stored frozen at -80°C .

Before an experiment, the protein was thawed and cycled through one round of Ca assembly and disassembly to remove any inactive protein. The protein was first dialyzed into 50 mM Mes, pH 6.5, 1 mM EGTA to remove KCl (two changes of buffer for 2 h each) and CaCl_2 was added to 10 mM and GTP to 2 mM. After five min at 37°C the FtsZ polymer was collected by centrifugation at 45,000 rpm, 30 min (TLA100 rotor, Beckman, Fullerton, CA). The pellet was resuspended in the appropriate buffer for the experiment at a protein concentration $>100\ \mu\text{M}$. Another centrifugation was done to remove any insoluble protein. The protein concentration was determined using a BCA assay and corrected for the 75% color ratio of FtsZ/BSA (Lu et al., 1998). Protein was normally used on the same day, but we found that it could be stored at 4°C for up to a week if the concentration was $>100\ \mu\text{M}$. We found that the protein lost assembly activity if diluted into buffer without potassium, so all storage buffers contained at least 100 mM KAc.

Buffers used

We studied assembly in several different buffers, which we designate by shorthand. All buffers contained 1 mM EGTA, and pH was adjusted with NaOH to avoid adding unknown amounts of potassium. The buffers are listed under Table 1.

The buffers were chosen for the following rationales. pH 7.7 is close to the physiological pH of *E. coli* cytoplasm, but pH 6.5 has been used for many assembly studies in vitro. Potassium is known to affect the assembly and GTPase of *E. coli* FtsZ, and has often been used at 100 mM, although 350 mM is closer to the physiological concentration (Cayley et al., 1991; Record et al., 1998). Assembly in Mg is accompanied by GTP hydrolysis, whereas in EDTA assembly occurs but hydrolysis is completely blocked.

Fluorescence measurements

Equilibrium fluorescence was measured with a SPEX Fluoromax spectrofluorometer (Jobin Yvon, Edison, NY), using a 4-mm inside diameter cylindrical quartz cell. The FtsZ-L68W was excited at 295 nm, using a slit width of 2.1 nm (the small slit was used to minimize bleaching). Fluorescence was monitored by an emission scan, or at the emission peak at 345–350 nm. For equilibrium measurements FtsZ was diluted to the appropriate concentration and GTP or GDP was added to a concentration of 200 μM . Readings were taken ~ 150 s after GTP addition, when the fluorescence was at a steady plateau.

Stopped-flow measurements were made using an 8100 spectrofluorometer (SLM-Aminco, Jobin Yuon, Edison, NY) equipped with the Milliflow Reactor stopped-flow accessory (SLM). The temperature was controlled at

TABLE 1 FtsZ-L68W Critical concentration determined by steady-state fluorescence in different buffers

	C_C (μM) from fluorescence	Slope*	C_C L68W from sediment†	C_C wt from sedimentation
pH 7.7				
HE	2.77 ± 0.3	17.7		
HEK100	0.45 ± 0.05	25.8		
HEK350	0.45 ± 0.05	27.0	0.3	
HM	0.30 ± 0.04	23.3		
HMK100	0.1 ± 0.01	24.5		1–1.25‡
HMK350	0.12 ± 0.05	25.9	0.1	
pH 6.5				
ME	0.46 ± 0.05	17.4	0.5	
MEK	0.36 ± 0.05	22.1		$\sim 4^{\S}$
MM	0.29 ± 0.08	13.7	0.2	
MMK	0.19 ± 0.06	22.8		0.9 ; 0.4 §

Buffers used: KAc, potassium acetate; MgAc, magnesium acetate. All buffers contained 1 mM EGTA; pH was adjusted with NaOH to avoid introducing uncontrolled amounts of potassium. (HE, 50 mM HEPES, pH 7.7, 2.5 mM EDTA; HEK100, 50 mM HEPES, pH 7.7, 100 mM KAc, 2.5 mM EDTA; HEK350, 50 mM HEPES, pH 7.7, 350 mM KAc, 2.5 mM EDTA; HM, 50 mM HEPES, pH 7.7, 5 mM MgAc; HMK100, 50 mM HEPES, pH 7.7, 100 mM KAc, 5 mM MgAc; HMK350, 50 mM HEPES, pH 7.7, 350 mM KAc, 5 mM MgAc; ME, 50 mM Mes, pH 6.5, 2.5 mM EDTA; MEK, 50 mM Mes, pH 6.5, 100 mM KAc, 2.5 mM EDTA; MM, 50 mM Mes, pH 6.5, 5 mM MgAc; MMK, 50 mM Mes, pH 6.5, 100 mM KAc, 5 mM MgAc.)

*Fluorescence was measured in arbitrary units, and can vary from day to day. All measurements for this table were obtained in one day, so the slopes (of the line above C_C) can be compared.

†These data were obtained by Mr. José González, as described in Gonzalez et al. (2003).

‡From sedimentation; González et al. (2003).

§ From calorimetry; Caplan and Erickson (2003).

||From sedimentation; Mukherjee and Lutkenhaus (1998). The C_C was reported to be 1.4 μM , based on the x -axis intercept, but we have corrected this for the 0.6 slope of the line.

25.0°C . One reactant syringe contained twice the indicated concentration of FtsZ and the other contained 400 μM GTP; they were mixed 1:1 to start the assembly reaction. Tryptophan fluorescence was excited at 295 nm and the emission intensity was monitored at 345 nm, both with a 4-nm slit. The total time of data collection was set to fully achieve the assembly plateau, and varied from 5 to 35 seconds depending on the protein concentration and the buffer. For each run we collected 200–250 data points. Four to five separate acquisitions were superimposed to confirm that they were identical, and were then averaged to produce the final data curve used in the global kinetic analysis. The protein concentration was initially calculated based on the dilution, and was adjusted so that the initial fluorescence values fell on a straight line (these adjustments, typically 1–2%, corrected for small pipetting errors).

Kinetic modeling

The minimal kinetic model postulates three steps after addition of GTP to FtsZ: activation of the FtsZ monomer; formation of a dimer nucleus; and elongation (see Scheme I, below). The first line indicates the activation step, the second line is the formation of the dimer nucleus, and the remaining lines are for elongation. Although elongation is written as multiple steps, the steps are actually identical, since we set all forward rate constants equal ($k_3 = k_4 = \dots = k_8 = k_c$) and all reverse rate constants equal ($k_{-3} = k_{-4} = \dots = k_{-8} = k_{-c}$), with the exception that k_{-7} was set equal to zero. The use of multiple

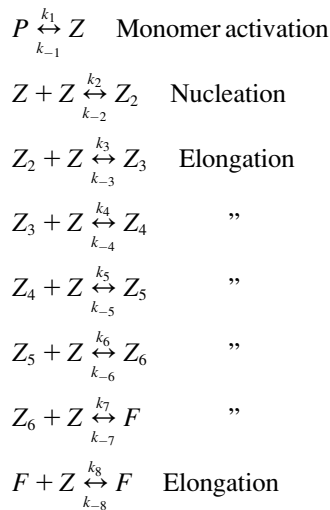
elongation steps and setting $k_{-7} = 0$ follow the procedure of Frieden and Goddette (1983): the multiple elongation steps are needed “to make the flux through the step before the final step independent of the nucleus size.” Setting $k_{-7} = 0$ ensures that one does not generate a buildup of Z_6 as the concentration of filaments increases. With $k_{-7} = 0$ we found that the kinetic constants did not change when we increased the number of elongation steps beyond seven. We also found that if we included 12–13 elongation steps, we did not need to set any k -value to zero.

The kinetic data were fit using the programs KINSIM40 and FITSIM40 (Barshop et al., 1983; Zimmerle and Frieden, 1989; Frieden, 1994; Dang and Frieden, 1997). The output from KINSIM was total tryptophan fluorescence defined as

$$\begin{aligned} Fls &= A_1 \times C_m + A_2 \times C_p + A_3 \\ &= A_1 \times C_m + A_2 \times (C_t - C_m) + A_3, \end{aligned}$$

where A_1 is the monomer fluorescence (which was determined from the initial fluorescence intensity at each concentration of FtsZ-L68W); C_m is the concentration of monomer at each time point in the simulation; A_2 is the fluorescence for protein in polymer (which was calculated from the plot of plateau fluorescence intensity at different FtsZ-L68W concentrations); C_p is the concentration of FtsZ-L68W in polymer at each time point; and $C_p = C_t - C_m$, where C_t is the total concentration of FtsZ. A_3 is a constant to account for the blank.

The FITSIM program has the potential to allow several kinetic constants to vary and seek the best global fit to the full set of kinetic curves. In practice, however, the program is unstable and crashes unless the input parameters are close to the final good fit. We began the process by fitting a single concentration, e.g., 1 μM , and allowing FITSIM to adjust two or more k -values at a time. When attempting a global fit to the eight or nine curves at different concentrations, we found it was best to allow the program to adjust only one variable at a time. We would then fix this value and allow the program to adjust another one. By successive approximations one gets closer and closer to a good fit to all the curves.



SCHEME I

RESULTS

Steady-state assembly

Fig. 1 shows the emission spectrum of FtsZ L68W excited at 295 nm. The broad emission with a peak at ~ 350 nm is characteristic of tryptophan in an aqueous environment. The

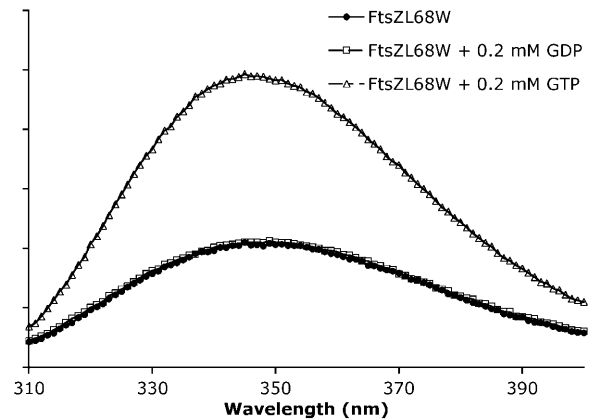


FIGURE 1 The tryptophan fluorescence emission spectrum of 0.5 μM FtsZ L68W in MMK buffer, excited at 295 nm, is shown before and after addition of 0.2 mM GDP and GTP.

fluorescence was unchanged when GDP was added. When GTP was added, there was an $\sim 250\%$ increase in fluorescence and this was accompanied by a small blue shift (Fig. 1). As discussed later we believe this fluorescence increase is due entirely to polymerization, and thus provides a direct measure of the amount of FtsZ in polymer.

We first studied assembly at pH 7.7, 100 mM KAc, in the absence of Mg (HEK buffer). Fig. 2 *a* shows a plot of fluorescence at 350 nm before and 150 s after addition of 200 μM GTP. For concentrations below 0.4 μM the two curves are superimposed, whereas above 0.4 μM the slope of the GTP curve is sharply higher. Fig. 2 *b* shows the fluorescence enhancement, calculated by subtracting the bottom curve from the GTP curve. This curve is typical of a cooperative assembly with a critical concentration (C_C) of 0.4 μM . Below the C_C there is no assembly at all, and above C_C all subunits assemble into polymer (Oosawa and Kasai, 1962).

We next repeated the experiment in the presence of Mg, where assembly is accompanied by GTP hydrolysis. Fig. 3 shows that under these conditions (HMK buffer) the C_C is significantly lowered, to ~ 0.1 μM .

The experiments in Figs. 1–3 were done in 100 mM KAc at pH 7.7. This is close to the physiological pH, but the KAc concentration is higher in the cytoplasm, near 350 mM at low osmotic conditions (Cayley et al., 1991; Record et al., 1998). We therefore examined the effect of potassium concentration by repeating the experiment with 0, 100, and 350 mM KAc. The C_C and slopes of the curves were identical at 100 and 350 mM potassium (Fig. 4). In the absence of potassium there was a very large increase in C_C , from 0.4 to 2.8 μM , indicating that the assembly was substantially weakened. In addition the slope of the line above the C_C was significantly reduced. A possible explanation for this reduction will be discussed below.

Many studies of FtsZ assembly have been done at pH 6.5, so we examined assembly at this lower pH, with and without

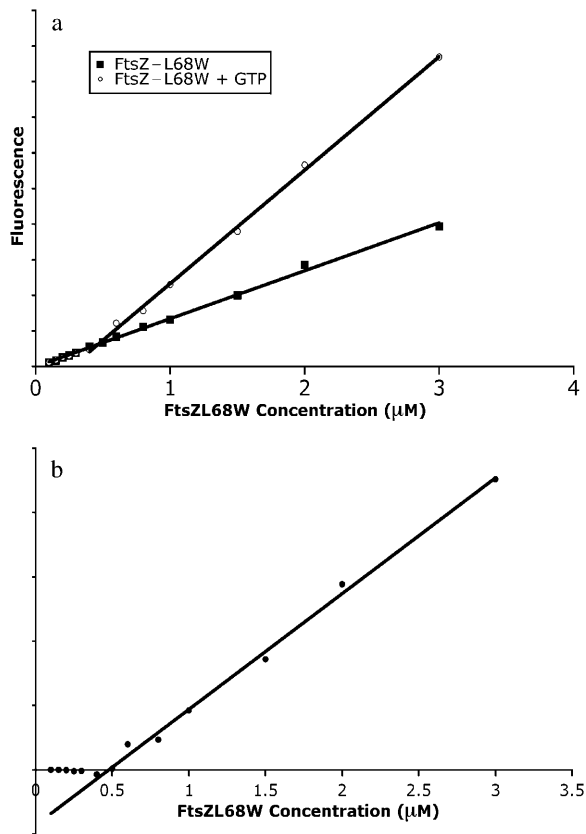


FIGURE 2 Fluorescence of L68W as a function of protein concentration, in HEK buffer, pH 7.7. (a) Fluorescence is shown for FtsZ before and 150 s after addition of GTP. (b) The no-GTP curve was subtracted from the GTP curve to show the fluorescence enhancement, which is interpreted to be the measure of total polymer. The C_C in this buffer, with no Mg, is $0.4 \mu\text{M}$.

Mg. These gave curves similar to those at pH 7.7, with C_C of $0.2 \mu\text{M}$ with Mg and $0.35 \mu\text{M}$ without Mg. We also examined the effect of potassium on assembly at pH 6.5. 100 mM KAc lowered the C_C and increased the slope of the line above C_C , similar to the results at pH 7.7. Data are collected in Table 1 for the different buffer conditions.

The C_C that we determined by fluorescence for L68W ($0.1 \mu\text{M}$ in HMK pH7.7) is significantly lower than the values of 1.0 – $1.25 \mu\text{M}$ obtained in previous studies of wild-type FtsZ (Gonzalez et al., 2003). Similarly, the C_C we measured in MEK pH 6.5 was $0.4 \mu\text{M}$ for L68W measured by fluorescence, versus $4 \mu\text{M}$ for wild-type FtsZ measured by calorimetry (Caplan and Erickson, 2003). We therefore wanted to determine whether the difference was due to the fluorescence assay or to the mutation. We performed a sedimentation assay of L68W in several buffers, exactly as described previously for wild-type FtsZ (Gonzalez et al., 2003). The C_C values from sedimentation were very close to those measured by the fluorescence assay for four different buffer conditions (Table 1), so we conclude that the C_C of L68W is actually 5–10 times lower than that of wild-type FtsZ. This was also confirmed by EM, where we observed

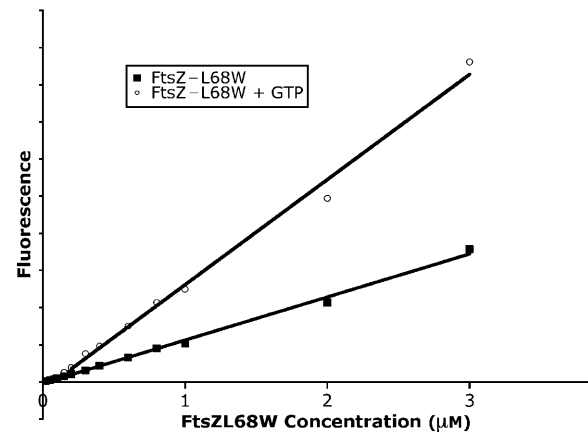


FIGURE 3 Assembly of L68W in HMK buffer, pH 7.7. The fluorescence for FtsZ-L68W before and 150 s after addition of GTP are shown. In this buffer, which contains Mg and permits GTP hydrolysis, the C_C was reduced to $0.1 \mu\text{M}$.

protofilaments of L68W assembled at $0.4 \mu\text{M}$ FtsZ in MEK buffer, and at $0.6 \mu\text{M}$ in HEK. These protofilaments were assembled just above the C_C that we determined for L68W, but well below the C_C for wild-type FtsZ.

The assembly products of L68W were examined by negative-stain electron microscopy (Fig. 5). The EM showed long thin protofilaments that are very similar to those of wild-type FtsZ. In particular they appear to be one-subunit thick. To confirm this we sent a sample of L68W to the scanning transmission electron microscope (STEM) facility at Brookhaven National Laboratory, repeating the mass analysis of our previous study (Romberg et al., 2001). The new study gave a mass per unit length of $0.79 \text{ Da}/\text{\AA}$, which is somewhat less than the $0.93 \text{ Da}/\text{\AA}$ expected for the one-subunit-thick protofilament. We conclude that under the

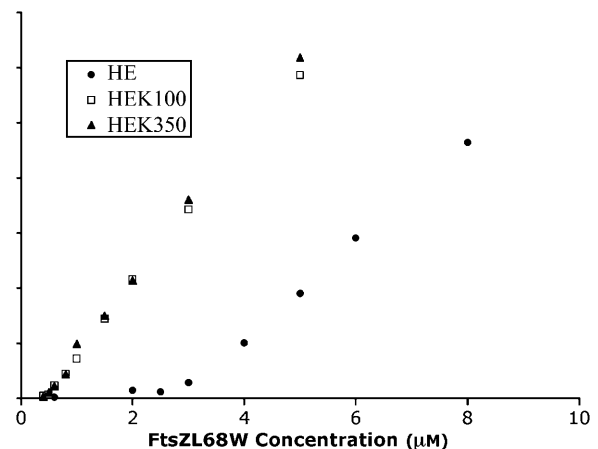


FIGURE 4 Assembly in HE buffer, pH 7.7, with variable concentrations of KAc. Assembly appeared to be identical in 100 and 350 mM KAc, with $C_C = 0.45 \mu\text{M}$. In the absence of potassium the C_C increased dramatically to $2.77 \mu\text{M}$, and the slope of the curve above C_C also decreased.

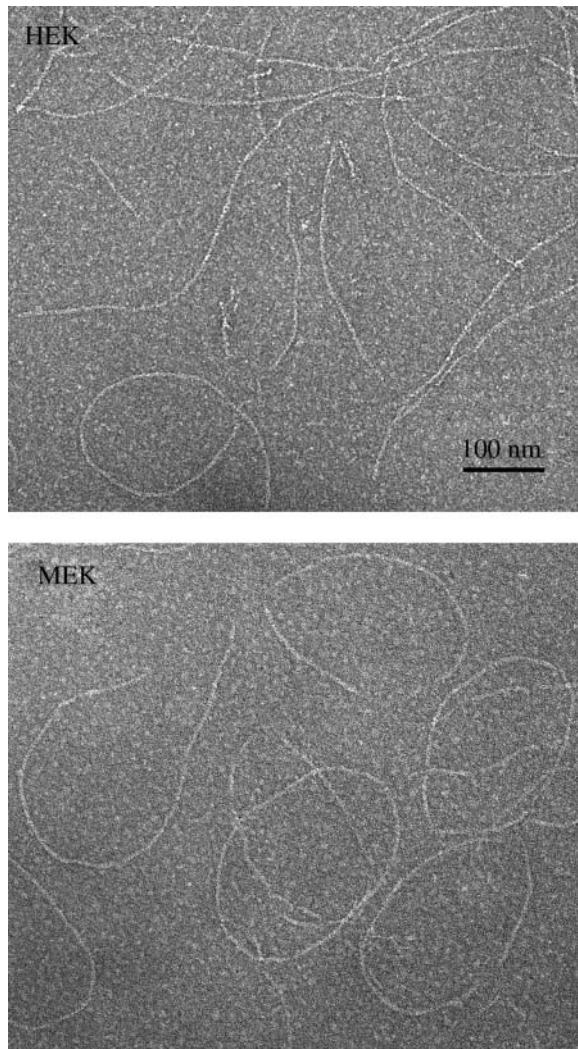


FIGURE 5 EM of FtsZ-L68W assembled at $1 \mu\text{M}$ protein for two min, in HEK and MEK buffers. The protofilaments appear to be one-subunit thick. They show a tendency to curve, forming circles $\sim 200\text{--}300$ nm in diameter. (This is quite different from the curved conformation, which forms rings and tubes of 23-nm diameter.)

conditions of our experiments the assembly is producing protofilaments that are one-subunit thick.

In HEK buffer the protofilaments ranged in length from 400 to 800 nm (100–200 subunits) after one or several minutes' assembly (Fig. 5). At earlier times the protofilaments were shorter. At 15 s, which is before the plateau is reached, protofilaments ranged from 20 to 100 subunits, with an average length of 60. Importantly, in HMK and $0.5 \mu\text{M}$ FtsZ, the protofilaments were much shorter, ranging from 10 to 30 subunits with an average length of 20. The length distribution for Mg assembly was essentially the same at 15 and 60 s. A curious feature of the L68W protofilaments is their tendency to curve. At the 2-min time point used for Fig. 2 some of the curved protofilaments in MEK buffer have formed circles $\sim 200\text{--}300$ nm in diameter. The circles

were not formed in the first 15 s, so this feature does not affect the kinetics over the period used for fitting (below).

In addition to the straight conformation, FtsZ protofilaments can exist in a curved conformation. This curved conformation is quite different from the gentle curvature described above, with a 22° bend between subunits producing rings or tubes of 23-nm diameter (Erickson et al., 1996; Lu et al., 2000). To determine whether the curved conformation gave a similar fluorescence increase, we studied assembly of FtsZ-L68W in MEK plus DEAE dextran (Lu et al., 2000). In GTP the protein ($0.04\text{--}0.12$ mg/ml FtsZ plus 0.05 mg/ml DEAE dextran) assembled into bundles of straight protofilaments, and these showed a substantial fluorescence increase. In GDP the protein assembled into tubes representing the curved conformation (Lu et al., 2000), but this assembly was not accompanied by a fluorescence increase. This suggests that the interface in the curved conformation is tilted in such a way as to prevent the tryptophan side chain from contacting the subunit above it.

To alleviate concerns about how the L68W mutation might alter assembly, we did some experiments in which L68W was mixed with an excess of wild-type FtsZ. When L68W was well below its C_C , assembly was only obtained when wild-type FtsZ was present above its C_C . Assembly gave a fluorescence increase similar to that of pure L68W. When L68W was below but closer to its C_C , the C_C of the mixture was between that of wild-type and L68W. The effect of L68W on C_C complicates its use in the mixtures, but with a sensitive fluorometer it may be useful as a tracer to study assembly of wild-type FtsZ.

Kinetics of assembly

We studied the kinetics of assembly using a stopped-flow device to mix GTP and FtsZ. Previous studies have indicated that this FtsZ, which had been assembled in calcium and resuspended with no added nucleotide, carries one molecule of bound GDP per FtsZ. All assembly curves showed a lag, followed by an increasing fluorescence, and finally a plateau. This is similar to curves for actin assembly, although on a much faster timescale (~ 10 s for FtsZ versus 1000 s for actin). The kinetic data were fit using the programs KINSIM40 and FITSIM40 (Barshop et al., 1983; Zimmerle and Frieden, 1989; Frieden, 1994; Dang and Frieden, 1997), with a mechanism similar to the nucleated assembly of actin (Frieden, 1983; Frieden and Goddette, 1983; Buzan and Frieden, 1996). We were able to obtain close fits to the experimental data with a reaction mechanism involving only three steps: monomer activation, a dimer nucleus, and elongation.

Experimentally we first studied assembly kinetics in HEK and MEK buffers, which are pH 7.7 and 6.5, respectively. These buffers lack Mg, and assembly occurs without GTP hydrolysis. Polymerization at pH 7.7 required ~ 30 s to reach a plateau at $1 \mu\text{M}$ FtsZ-L68W, but only ~ 6 s at $4.8 \mu\text{M}$ (Fig.

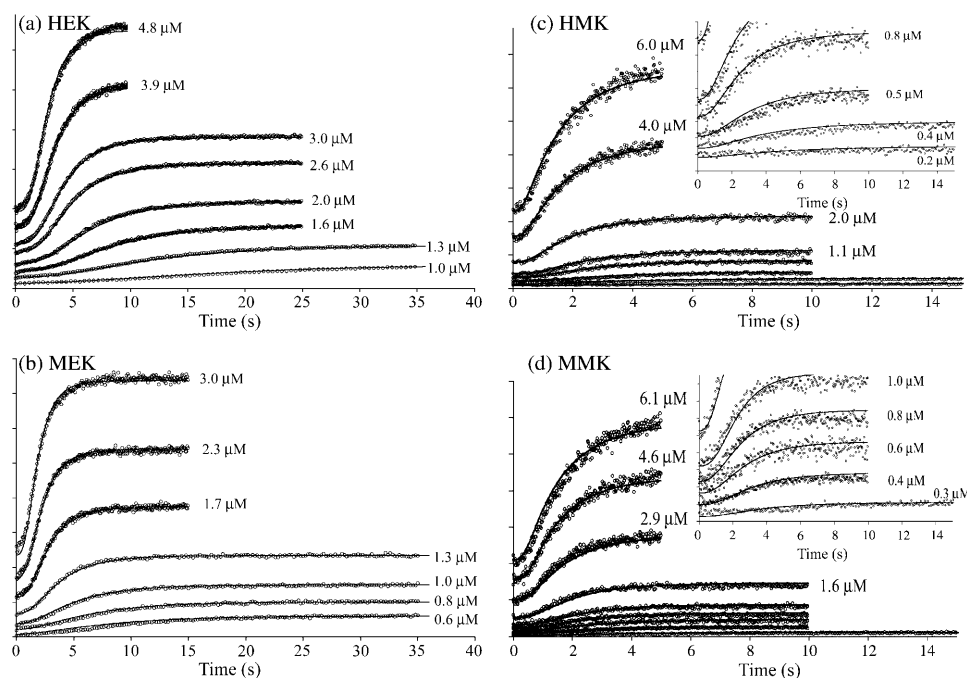


FIGURE 6 Stopped-flow data (circles) and the best fit from KINSIM (lines) for assembly in different buffers. The insets in *c* and *d* show the lower concentrations on an expanded scale. The concentration of FtsZ is indicated by each curve.

6). Assembly was faster at pH 6.5. The fluorescence increased 2.3-fold in both buffers at the highest protein concentrations. The C_C values determined from the stopped-flow experiment were close to the values determined from equilibrium fluorescence measurements (Table 1).

We next studied assembly kinetics in HMK and MMK buffers, which contain 2.5 mM Mg, permitting GTP hydrolysis. Assembly was much faster in Mg than in EDTA buffer, reaching a plateau in 10 s even at the lowest protein concentrations (Fig. 6, *c* and *d*).

For each of the four buffers, we were able to achieve a global fit of the assembly curves at the 7–9 different concentrations. Assembly in all buffers was fit with the same mechanism (Scheme I; see also Fig. 7), but the kinetic constants giving the best fit varied considerably for the different buffers. The kinetic constants for the best fits are collected in Table 2 and are discussed below.

DISCUSSION

Steady-state assembly

E. coli FtsZ has no natural tryptophan residues and only two tyrosines, so the 68W introduced in our mutant provides the sole source of fluorescence at 350 nm when excited at 295 nm. L68 is located on the upper surface of FtsZ, a short distance from the β -phosphate of the GDP. The enhanced affinity (lower C_C) of the L68W mutant relative to wild-type FtsZ suggests that the Trp makes contact with the subunit above it in the protofilament and contributes some buried surface and hence binding energy to the interface. The enhanced affinity raised the concern that the assembly of the

L68W mutant might be different from that of wild-type FtsZ, but this is alleviated by the observation that the protofilaments assembled are very similar, and that the mutant protein can function for cell division as the sole source of FtsZ (S. D. Redick, J. Stricker, G. Briscoe, and H. P. Erickson, unpublished).

We have interpreted the fluorescence enhancement as due to polymerization, but another possibility is a conformational change in the FtsZ caused by GTP binding. In fact, Diaz et al. (2001) observed a 30% fluorescence enhancement upon GTP addition for a similar mutant (*Methanococcus jannaschii* FtsZ T92W) and interpreted it as due to a conformational change within monomeric FtsZ. The equivalent mutation in *E. coli* would be T65W. T65 and L68 are three residues apart in the linear sequence, but they are actually adjacent to each other in the three-dimensional structure. The two tryptophan mutations, although very close in the structure, appear to change fluorescence in response to different environmental changes.

Our interpretation that the fluorescence enhancement of *E. coli* L68W is due to assembly, not to GTP binding, is supported by several observations. First, at protein concentrations below C_C the fluorescence curves are identical with GTP and GDP. Thus the fluorescence enhancement correlates with assembly, which occurs only above C_C , and not with GTP binding, which also should occur below C_C . Finally, the kinetics of the fluorescence change monitored by stopped flow showed a strong dependence on protein concentration and time, which can only be explained by a nucleated assembly reaction.

The different buffer conditions resulted in different C_C , but they also gave different slopes of the line above C_C . Above

TABLE 2 FtsZ-L68W assembly rate constants at four different buffers

	k_1 (s^{-1})	k_{-1} (s^{-1})	k_2 ($\mu M^{-1}s^{-1}$)	k_e ($\mu M^{-1}s^{-1}$)	k_{-2} (s^{-1})	k_{-e} (s^{-1})	k_{-2}/k_2 (μM)	k_{-e}/k_e (μM)
HEK	1.1	0.01	4.2	5.1	7700	2.9	1850	0.56
MEK	1.3	0.01	4.3	4.6	460	1.85	107	0.4
HMK	0.70	0.04	1.0	3.6	1.2	0.36	1.21	0.10
MMK	0.76	0.11	0.62	3.0	0.30	0.60	0.47	0.20

The values k_1 and k_{-1} are the parameters for monomer activation; k_2 and k_{-2} are for formation of the dimer nucleus; and k_e and k_{-e} are for elongation.

C_C all additional subunits should polymerize, regardless of what the C_C is, so the change in slope in the different buffers was surprising. A likely explanation is that the different buffers affect the structure of the interface, and slightly change the interaction of 68W with the subunit above it.

Kinetic analysis and the nucleation mechanism

The kinetics of assembly were measured in four different buffers. The same reaction mechanism (see Scheme I; see also Fig. 7) was used to fit the data in each buffer, but the kinetic constants giving the best fit varied considerably (Table 2). The reaction mechanism had three steps: 1), activation of the FtsZ monomer after GTP addition; 2) a dimer nucleation step; and 3), elongation. We will focus our discussion initially on the EDTA buffers, where the assembly is not complicated by GTP hydrolysis, and may therefore be considered a reversible reaction.

A potential complication of the kinetic studies is that FtsZ tends to form oligomers even in GDP (Mukherjee et al., 1993; Sosson et al., 1999; Justice et al., 2000; Rivas et al., 2000). These GDP oligomers are substantially weaker than assembly in GTP, and are dependent on Mg (Rivas et al., 2000). They should not exist for assembly in EDTA, and this is where we see the clearest evidence for a weak dimer nucleus. At the 5 mM Mg concentration in our buffers the K_D for GDP association is 4 μM (or 8 μM if one corrects for bidirectional growth; Romberg et al., 2001; Rivas et al., 2000). The highest concentrations in our kinetic study were 6 μM , so these curves might be affected by GDP dimerization, if these dimers can be converted directly into GTP dimers. If GDP dimers first have to dissociate before reassembling in GTP they may contribute little. The possible contribution of GDP dimers to the assembly kinetics should be kept in mind and addressed in future studies.

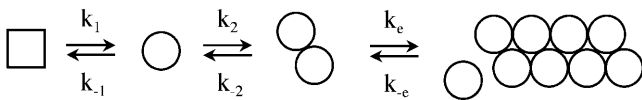


FIGURE 7 The model used to fit the stopped-flow kinetic data. The first step is monomer activation, probably dissociation of the bound GDP. This is followed by formation of a weak dimer nucleus, and then by steps of elongation. The model shows the polymer as a two-stranded filament because this is the simplest explanation for a dimer nucleus, but this is contradicted by the EM, which shows FtsZ protofilaments to be single-stranded.

The first step in the assembly mechanism is monomer activation. This is needed to account for the lag of ~ 1 s, which remains even at the highest FtsZ concentrations. The KINSIM fitting gave very similar values, 1.1–1.3 s^{-1} , for the two EDTA buffers, and a somewhat faster 0.7 s^{-1} in Mg. There are several possibilities for what the activation might involve. The one we favor is that 1 s is the time required for release of bound GDP, which must occur before GTP can be bound. The kinetics of nucleotide binding and exchange have not been studied, and there are conflicting data for the K_D for binding. This will need to be addressed in a future kinetic study.

We will next discuss the elongation phase of the reaction. The diffusion-limited association rate for a large number of protein-protein associations is $\sim 2\text{--}5 \mu M^{-1}s^{-1}$ (Northrup and Erickson, 1992). We started the fitting by setting k_e to 2, but found that 5 $M^{-1}s^{-1}$ gave a better fit, so this was used for subsequent steps. We then set the reverse rate constant $k_{-e} = 5/C_C$, to give the measured C_C . After optimizing all parameters, k_e varied only slightly for the four different buffers, from 3 to 5 $\mu M^{-1}s^{-1}$, and k_{-e} varied from 0.3 to 3 s^{-1} , reflecting the variation in C_C . Note that the last column in Table 2, k_{-e}/k_e , should equal C_C for each buffer. The best fit values from the kinetics study are close to those determined from equilibrium measurements in Table 1.

Finally, we will address the nucleation step. For actin assembly, nucleation involved two species, a dimer and a trimer (and in some cases a monomer nucleation step; Cooper et al., 1983a; Frieden and Goddette, 1983; Tobacman and Korn, 1983). For FtsZ assembly we found that a dimer nucleus was needed, but there was no need for a trimer. Adding a trimer nucleus and adjusting its kinetic parameters gave no improvement in fit. As expected for a nucleus the dimer is weak, with $K_D = k_{-2}/k_2 = 1850 \mu M$ in HEK and 107 μM in MEK. The dimer nucleus is thus 3300, and is 260 times weaker than the elongation step (k_{-e}/k_e). (For actin the dimer was much weaker, with $K_D = 8 \times 10^5 \mu M$. This is the reason that actin assembly is 100 times slower than FtsZ.) Interestingly, the forward rate constant for forming the dimer was 4 $M^{-1}s^{-1}$, essentially the same as the diffusion-limited rate for elongation. The weakness of the dimer is due entirely to its rapid dissociation rate.

In Mg buffers the monomer activation appears to be somewhat faster, which may reflect a role for Mg in the nucleotide exchange. The kinetics of the elongation step are similar to those in EDTA, with a k_e of 3–3.6 $M^{-1}s^{-1}$. The

value k_{-e} is smaller in Mg, reflecting the lower C_C (but see the caution below).

The one step that is strikingly different in Mg and EDTA is the formation of the dimer nucleus. In Mg the k_2 for formation of the dimer is somewhat lower, but the dissociation rate, k_{-2} , is more than three orders-of-magnitude lower. This means that the dimer nucleus in Mg is much more stable than in EDTA, and indeed it appears to be only 10- or 2.3-fold weaker than the elongation step. However, this raises an important caution. The C_C for elongation in Mg is not a true C_C because we have ignored the role of GTP hydrolysis. Hydrolysis occurs at a rate of 8 min^{-1} in MMK (Romberg and Mitchison, 2004), so it should not be a factor in the nucleation and early elongation stages of the reaction. Hydrolysis should, however, play a major role as the reaction approaches the plateau. In particular, the fitted parameter k_{-e} will have a small contribution from dissociation of FtsZ-GTP subunits, but will probably be dominated by dissociation of FtsZ-GDP after GTP hydrolysis. The equilibrium K_D for the elongation reaction will actually be much smaller than the k_{-e}/k_e obtained from the fitting (Table 1). This means that elongation of FtsZ-GTP filaments is actually much stronger, relative to nucleation, than indicated by the numbers in Table 1.

Fragmentation/annealing—is it important in FtsZ assembly?

An important feature implicit in the nucleation model is that assembly and disassembly occur only at the ends of protofilaments, and no steps of fragmentation and annealing are needed to obtain the excellent global fit. This means that fragmenting a filament in the middle is highly unfavorable relative to end dissociation, which is another hallmark feature of cooperative assembly (Erickson, 1989). Although fragmentation/annealing is not needed for the global fit, it is still important to consider whether it might occur. Fragmentation has been included in models for some actin studies (Cooper et al., 1983a; Tobacman and Korn, 1983), where it improved the global fit significantly. The excellent fit that we obtain without it probably means that fragmentation is insignificant in the time course of our assembly reactions. Annealing has been ignored in the actin field until recently. Sept et al. (1999) found that annealing was actually quite significant in actin assembly, and played a major role in determining the distribution of actin filament lengths. We can address the potential importance of annealing in FtsZ assembly with two approximate calculations.

We found by EM that protofilaments are 20–100 subunits long after ~ 15 s assembly in HEK buffer (somewhat before the plateau). Assuming our modeled rate constant of $5 \times 10^6 \text{ M}^{-1}\text{s}^{-1}$, and a starting subunit concentration of $1 \mu\text{M}$, filaments could grow at a maximum rate of 5 subunits per second, or 75 subunits in 15 s. The lengths should actually be lower because the free subunit concentration will drop to $0.45 \mu\text{M}$ as the assembly reaches the plateau, and filaments

nucleated later in the time course will be shorter. The observed distribution of lengths is therefore somewhat higher than the predicted maximum, suggesting that annealing may occur, although only a small amount.

An alternative approach is to calculate the fastest possible rate of annealing. At the assembly plateau the average filament length was 60 subunits, and the polymer mass was $0.55 \mu\text{M}$ (subtracting the C_C from the $1\text{-}\mu\text{M}$ total concentration). This means that the concentration of protofilaments is $\sim 9 \text{ nM}$ at the plateau. If we assume that protofilaments anneal at the diffusion-limited rate for single subunits, $5 \times 10^6 \text{ M}^{-1}\text{s}^{-1}$, any given protofilament would anneal with another one at a rate of $9 \times 10^{-9} \times 5 \times 10^6 = 0.045 \text{ s}^{-1}$, or one annealing event every 20 s. This is a maximum estimate of the rate of annealing events at the assembly plateau, and two factors will reduce it. First, the diffusion-limited association rate is reduced as filaments grow longer (Sept et al., 1999). Second, the concentration of filaments will be lower earlier in the assembly time. Thus the kinetics may be too slow for significant annealing in the 15-s assembly time.

These two arguments are ambiguous over whether annealing should be a factor in FtsZ assembly, so the possibility remains open. If annealing did occur it would reduce the concentration of filament ends, and this should affect the kinetics in a complex way. The exceptionally good global fit to the simple nucleation-elongation model would suggest that annealing is not significant, or if it occurs there must be some additional mechanism that exactly compensates for it.

Assembly in HMK, which contains Mg and permits GTP hydrolysis, gave a filament distribution after 15 s that was three times shorter than in EDTA. Moreover, these filaments did not grow longer by 60 s, so this distribution seems to be a steady-state phenomenon. Annealing is less likely to be a factor here than in the EDTA assembly. Fragmentation is a possibility, and this could be related to GTP hydrolysis. The steady-state distribution of filament lengths will depend on the mechanism of assembly dynamics coupled to GTP hydrolysis. This could include mechanisms like dynamic instability, treadmilling, and fragmentation, which are completely unknown at present.

Finally, we should emphasize that the model used is a minimal model, giving a good global fit to kinetics at different concentrations. Despite the good fit, this type of analysis cannot exclude more complex mechanisms, such as fragmentation/annealing. If new approaches demonstrate that additional mechanisms are important, the model will need to be adjusted to include them.

Cooperative assembly—resolutions and enigmas

Our lab has proposed that assembly of FtsZ may be isodesmic rather than cooperative, primarily on the basis that the protofilaments were measured to be only one-subunit thick (Romberg et al., 2001). In an isodesmic polymer, subunits are connected linearly by the same type of bond;

removing a subunit from the end is thermodynamically equivalent to fragmentation between any pair of subunits. Cooperative polymers like actin are based on two types of bonds connecting subunits into a helix or two-dimensional polymer (Oosawa and Kasai, 1962; Erickson, 1989). Removing a subunit from an end is orders-of-magnitude more favorable than fragmentation, because fragmentation involves breaking an additional bond. Several studies have concluded that FtsZ assembly produces pairs or bundles of protofilaments, and that this is the basis for cooperative assembly (Mingorance et al., 2001; Huecas and Andreu, 2003; Oliva et al., 2003). However, most of these images show some apparently single protofilaments, and these are the predominant structures formed in our assays. This suggests that the single protofilament is the basic structure, and that pairs and bundles are formed subsequently but are not an essential step in polymerization.

Several assays of FtsZ activity have reported a critical concentration, which is a hallmark of cooperative assembly. Perhaps most convincing are GTPase assays, which show a complete lack of hydrolysis below $C_C = \sim 1 \mu\text{M}$, and a rapid rise in activity at higher concentrations (Wang and Lutkenhaus, 1993; Oliva et al., 2003; Romberg and Mitchison, 2004). Light scattering, sedimentation, and calorimetry have also indicated a C_C (Mukherjee and Lutkenhaus, 1998, 1999; White et al., 2000; Caplan and Erickson, 2003; Gonzalez et al., 2003; Huecas and Andreu, 2003; Oliva et al., 2003). We have previously expressed concern that sedimentation and light scattering would underestimate small polymers and that bundling of protofilaments would skew the assay. The fluorescence assay that we report here is simply proportional to the number of subunits forming protofilament interfaces, and should not be affected by polymer size or bundling.

The agreement of our fluorescence assay with previous studies by light scattering suggests a feature of assembly not previously noted. One might have expected that as the total protein concentration increased, the protofilaments would become longer and/or would form increasingly large bundles. However, the light scattering signal appears strikingly linear in several independent studies of *E. coli* FtsZ (Mukherjee and Lutkenhaus, 1998; Gonzalez et al., 2003), and a similar linearity was reported for FtsZ from *Mycobacterium tuberculosis* (White et al., 2000) and *M. jannaschii* (Oliva et al., 2003). This must mean that the protofilaments are of the same average length regardless of the total protein concentration, and they do not increase their tendency to bundle at higher concentrations. The agreement of light scattering, sedimentation, and our fluorescence assay now validates all three and provides this new insight on the uniformity of the polymers.

We believe that the excellent fit of the kinetic data to the dimer nucleation model, and the absence of fragmentation, provides a definitive argument that FtsZ assembly is cooperative, not isodesmic. This leaves us with an enigma—how can a protofilament that is one-subunit thick produce cooperative assembly? One possible resolution would be to

propose that appearance from negative-stain EM and the mass measurements by STEM are wrong, and the protofilaments are actually two-subunits thick. However, the historical accuracy of the STEM for mass measurement is excellent, and it is difficult to imagine it being off by a factor of 2. An alternative would be to propose some structural feature within the one-subunit-thick protofilament that provides the equivalent of two types of bonds. We have not come up with any plausible model, so for the moment we have to leave this as an enigma.

The fluorescence assay using *E. coli* FtsZ L68W is a simple and direct assay for studying FtsZ assembly. We have applied it here to investigate the thermodynamics and kinetics in four different buffers. It should also be useful in screening compounds that interfere with FtsZ assembly and thereby block bacterial cell division.

We thank Mr. José González, Centro de Investigaciones Biológicas, Madrid, for determination of C_C by sedimentation; and we thank Ms. Martha Simon and Dr. James Hainfeld, Brookhaven National Laboratory, for performing the mass analysis of L68W protofilaments by scanning transmission electron microscope.

Supported by National Institutes of Health grant GM66014 to H.P.E.

REFERENCES

- Anderson, D. E., F. J. Gueiros-Filho, and H. P. Erickson. 2004. Assembly dynamics of FtsZ rings in *Bacillus subtilis* and *Escherichia coli* and effects of FtsZ-regulating proteins. *J. Bacteriol.* 186:5775–5781.
- Barshop, B. A., R. F. Wrenn, and C. Frieden. 1983. Analysis of numerical methods for computer simulation of kinetic processes: development of KINSIM—a flexible, portable system. *Anal. Biochem.* 130:134–145.
- Buzan, J. M., and C. Frieden. 1996. Yeast actin: polymerization kinetic studies of wild-type and a poorly polymerizing mutant. *Proc. Natl. Acad. Sci. USA.* 93:91–95.
- Caplan, M., and H. P. Erickson. 2003. Apparent cooperative assembly of the bacterial cell-division protein FtsZ demonstrated by isothermal titration calorimetry. *J. Biol. Chem.* 278:13784–13788.
- Cayley, S., B. A. Lewis, H. J. Guttman, and M. T. Record, Jr. 1991. Characterization of the cytoplasm of *Escherichia coli* K-12 as a function of external osmolarity: implications for protein-DNA interactions in vivo. *J. Mol. Biol.* 222:281–300.
- Cooper, J. A., E. L. Buhle, S. B. Walker, T. Y. Tsong, and T. D. Pollard. 1983a. Kinetic evidence for a monomer activation step in actin polymerization. *Biochemistry.* 22:2193–2202.
- Cooper, J. A., S. B. Walker, and T. D. Pollard. 1983b. Pyrene actin: documentation of the validity of a sensitive assay for actin polymerization. *J. Muscle Res. Cell Motil.* 4:253–262.
- Dang, Q., and C. Frieden. 1997. New PC versions of the kinetic-simulation and fitting programs, KINSIM and FITSIM. *Trends Biochem. Sci.* 22: 317.
- Diaz, J. F., A. Kralicek, J. Mingorance, J. M. Palacios, M. Vicente, and J. M. Andreu. 2001. Activation of cell division protein FtsZ. Control of switch loop T3 conformation by the nucleotide γ -phosphate. *J. Biol. Chem.* 276:17307–17315.
- Erickson, H. P. 1989. Cooperativity in protein-protein association: the structure and stability of the actin filament. *J. Mol. Biol.* 206:465–474.
- Erickson, H. P., D. W. Taylor, K. A. Taylor, and D. Bramhill. 1996. Bacterial cell division protein FtsZ assembles into protofilament sheets and mini-rings, structural homologs of tubulin polymers. *Proc. Natl. Acad. Sci. USA.* 93:519–523.

- Frieden, C. 1983. Polymerization of actin: mechanism of the Mg^{2+} -induced process at pH 8 and 20°C. *Proc. Natl. Acad. Sci. USA.* 80:6513–6517.
- Frieden, C. 1994. Analysis of kinetic data: practical applications of computer simulation and fitting programs. *Methods Enzymol.* 240:311–322.
- Frieden, C., and D. W. Goddette. 1983. Polymerization of actin and actin-like systems: evaluation of the time course of polymerization in relation to the mechanism. *Biochemistry.* 22:5836–5858.
- Gonzalez, J. M., M. Jimenez, M. Velez, J. Mingorance, J. M. Andreu, M. Vicente, and G. Rivas. 2003. Essential cell division protein FtsZ assembles into one monomer-thick ribbons under conditions resembling the crowded intracellular environment. *J. Biol. Chem.* 278:37664–37671.
- Huecas, S., and J. M. Andreu. 2003. Energetics of the cooperative assembly of cell division protein FtsZ and the nucleotide hydrolysis switch. *J. Biol. Chem.* 278:46146–46154.
- Justice, S. S., J. Garcia-Lara, and L. I. Rothfield. 2000. Cell division inhibitors SulA and MinC/MinD block septum formation at different steps in the assembly of the *Escherichia coli* division machinery. *Mol. Microbiol.* 37:410–423.
- Kouyama, T., and K. Mihashi. 1981. Fluorimetry study of *N*-(1-pyrenyl)iodoacetamide-labelled F-actin. Local structural change of actin protomer both on polymerization and on binding of heavy meromyosin. *Eur. J. Biochem.* 114:33–38.
- Levin, P. A., and R. Losick. 1996. Transcription factor Spo0A switches the localization of the cell division protein FtsZ from a medial to a bipolar pattern in *Bacillus subtilis*. *Genes Dev.* 10:478–488.
- Lu, C., J. Stricker, and H. P. Erickson. 1998. FtsZ from *Escherichia coli*, *Azotobacter vinelandii*, and *Thermotoga maritima*—quantitation, GTP hydrolysis, and assembly. *Cell Motil. Cytoskeleton.* 40:71–86.
- Lu, C. L., M. Reedy, and H. P. Erickson. 2000. Straight and curved conformations of FtsZ are regulated by GTP hydrolysis. *J. Bacteriol.* 182:164–170.
- Ma, X., D. W. Ehrhardt, and W. Margolin. 1996. Colocalization of cell division proteins FtsZ and FtsA to cytoskeletal structures in living *Escherichia coli* cells by using green fluorescent protein. *Proc. Natl. Acad. Sci. USA.* 93:12998–13003.
- Mingorance, J., S. Rueda, P. Gomez-Puertas, A. Valencia, and M. Vicente. 2001. *Escherichia coli* FtsZ polymers contain mostly GTP and have a high nucleotide turnover. *Mol. Microbiol.* 41:83–91.
- Mukherjee, A., K. Dai, and J. Lutkenhaus. 1993. *Escherichia coli* cell division protein FtsZ is a guanine nucleotide binding protein. *Proc. Natl. Acad. Sci. USA.* 90:1053–1057.
- Mukherjee, A., and J. Lutkenhaus. 1998. Dynamic assembly of FtsZ regulated by GTP hydrolysis. *EMBO J.* 17:462–469.
- Mukherjee, A., and J. Lutkenhaus. 1999. Analysis of FtsZ assembly by light scattering and determination of the role of divalent metal cations. *J. Bacteriol.* 181:823–832.
- Northrup, S. H., and H. P. Erickson. 1992. Kinetics of protein-protein association explained by Brownian dynamics computer simulation. *Proc. Natl. Acad. Sci. USA.* 89:3338–3342.
- Oliva, M. A., S. Huecas, J. M. Palacios, J. Martin-Benito, J. M. Valpuesta, and J. M. Andreu. 2003. Assembly of archaeal cell division protein FtsZ and a GTPase-inactive mutant into double-stranded filaments. *J. Biol. Chem.* 278:33562–33570.
- Oosawa, F., and M. Kasai. 1962. A theory of linear and helical aggregations of macromolecules. *J. Mol. Biol.* 4:10–21.
- Record, M. T., Jr., E. S. Courtenay, S. Cayley, and H. J. Guttman. 1998. Biophysical compensation mechanisms buffering *E. coli* protein-nucleic acid interactions against changing environments. *Trends Biochem. Sci.* 23:190–194.
- Rivas, G., A. Lopez, J. Mingorance, M. J. Ferrandiz, S. Zorrilla, A. P. Minton, M. Vicente, and J. M. Andreu. 2000. Magnesium-induced linear self-association of the FtsZ bacterial cell division protein monomer—the primary steps for FtsZ assembly. *J. Biol. Chem.* 275:11740–11749.
- Romberg, L., and T. J. Mitchison. 2004. Rate-limiting guanosine 5'-triphosphate hydrolysis during nucleotide turnover by FtsZ, a prokaryotic tubulin homologue involved in bacterial cell division. *Biochemistry.* 43:282–288.
- Romberg, L., M. Simon, and H. P. Erickson. 2001. Polymerization of FtsZ, a bacterial homolog of tubulin. Is assembly cooperative? *J. Biol. Chem.* 276:11743–11753.
- Sept, D., J. Xu, T. D. Pollard, and J. A. McCammon. 1999. Annealing accounts for the length of actin filaments formed by spontaneous polymerization. *Biophys. J.* 77:2911–2919.
- Sosson, T. M., M. R. Brigham-Burke, P. Hensley, and K. H. Pearce. 1999. Self-activation of guanosine triphosphatase activity by oligomerization of the bacterial cell division protein FtsZ. *Biochemistry.* 38:14843–14850.
- Stricker, J., and H. P. Erickson. 2003. In vivo characterization of *Escherichia coli* FtsZ mutants: effects on Z-ring structure and function. *J. Bacteriol.* 185:4796–4805.
- Sun, Q., and W. Margolin. 1998. FtsZ dynamics during the division cycle of live *Escherichia coli* cells. *J. Bacteriol.* 180:2050–2056.
- Tobacman, L. S., and E. D. Korn. 1983. The kinetics of actin nucleation and polymerization. *J. Biol. Chem.* 258:3207–3214.
- Trusca, D., and D. Bramhill. 2002. Fluorescent assay for polymerization of purified bacterial FtsZ cell-division protein. *Anal. Biochem.* 307:322–329.
- Wang, X., and J. Lutkenhaus. 1993. The FtsZ protein of *Bacillus subtilis* is localized at the division site and has GTPase activity that is dependent upon FtsZ concentration. *Mol. Microbiol.* 9:435–442.
- White, E. L., L. J. Ross, R. C. Reynolds, L. E. Seitz, G. D. Moore, and D. W. Borhani. 2000. Slow polymerization of *Mycobacterium tuberculosis* FtsZ. *J. Bacteriol.* 182:4028–4034.
- Zimmerle, C. T., and C. Frieden. 1989. Analysis of progress curves by simulations generated by numerical integration. *Biochem. J.* 258:381–387.